UNITED NATIONS UNIVERSITY
UNU-GTP
Geothermal Training Programme

Orkustofnun, Grensasvegur 9,
IS-108 Reykjavik, Iceland

Reports 2017
Number 26

METAL SULPHIDE SCALING IN PRODUCTION WELLS IN AHUACHAPAN GEOTHERMAL FIELD, EL SALVADOR

Briseida G. Salazar Artiga
LaGeo S.A de C.V
15 Avenida Sur, Colonia Utila
Santa Tecla, La Libertad
EL SALVADOR C.A.
bsalazar@lageo.com.sv

ABSTRACT

Ahuachapán geothermal field has been exploited since 1975. For some of the production wells, deposits have been observed in separators during maintenance breaks of the power plant. X-ray diffraction analysis showed that these deposits were mainly composed of sulphide minerals. In this study, geothermal water collected on surface was used to determinate the saturation state of sulphide minerals such as bornite, chalcopyrite, pyrite, chalcocite, covellite, galena, pyrrhotite, and sphalerite. The selection of the minerals included in the study is based on geological reports. The reconstruction of fluid at reservoir conditions was done by using the WATCH program, as were steam fractions resulting from adiabatic boiling of the reservoir fluid. The saturation state of sulphide minerals was modelled by using the SOLMINEQ.88 program.

The results of the simulation show that pyrite and chalcopyrite are expected to be saturated under reservoir conditions in the wells that were considered in this study. Both minerals become super-saturated during the boiling process until the separator temperature is reached. Covellite, bornite, chalcocite, and galena were under-saturated at reservoir conditions but during the boiling process they become saturated. Pyrrhotite and sphalerite were under-saturated in all cases and therefore have no possibility of scaling neither under reservoir conditions nor in the boiling process.

1. INTRODUCTION

Generally, one of the principal problems during geothermal exploitation is scale deposition. High concentrations of dissolved mineral species combined with large changes in temperature or pressure conditions create scaling risk during plant operation (Banks, 2013). The formation of scales on the surfaces of equipment, in the casing or inside the reservoir can have serious economic consequences. The most common scaling problems are calcite and amorphous silica and both have been very well documented. A less common class of scale is heavy metal sulphides.

Understanding how and why sulphides precipitate is commonly quite complex. Chemical species containing metals and sulphides must be taken into account. In a natural environment, the chemical and

physical factors of sulphite precipitation are a response to a wide range of processes, such as temperature and fluid pressure, the history of water-rock interactions and operating conditions (Andritsos and Karabelas, 1991).

In saline, high enthalpy geothermal systems, we find diverse heavy metal sulphides in scale deposits such as PbS, ZnS, FeS, etc. Usually these scale deposits are mixed with other types of deposits such as amorphous silica or metallic silicates (especially iron) (Andritsos and Karabelas, 1995; Hardardóttir, 2011). Several geochemical programs have been developed to help predict scaling risks. This is done by calculating the chemical speciation at specified conditions of temperature and pressure and using solubility data to estimate the saturation levels of the relevant scaling minerals.

The main purpose of this report is to present an overview of sulphide scaling in production wells in the Ahuachapán geothermal field and to propose a methodology for predicting sulphide scales from the chemical composition of the well fluid.

2. DESCRIPTION OF AHUACHAPAN GEOTHERMAL FIELD

2.1 General information

El Salvador, which is commonly called the Land of Volcanoes, is located in Central America at the coast of the Pacific Ocean. It is characterized by major hydrothermal areas, hot springs and fumaroles. Earthquakes and other seismic activities occur frequently because it is situated above a large tectonic boundary. The high-temperature geothermal fields in El Salvador are associated with this volcanism.

At present, El Salvador has two geothermal energy production fields: Ahuachapán and Berlin (Figure 1). Ahuachapán geothermal field is located in the western part of the country, about 100 km west of San Salvador and 6 km from Ahuachapán city, and it has been exploited since 1975. It was one of the first geothermal resources utilized to produce power in a developing country. Ahuachapán has a production area of approximately 5 km^2 (Figure 2).

FIGURE 1: Location of geothermal plants in El Salvador

The temperature of the reservoir is in the range of 210-230°C (Julio Quijano, Reservoir engineer, LaGeo S.A de C.V., personal communication, October 5th, 2017) and the average reservoir pressure is about 19 bar-a (LaGeo, 2017a). Fifty wells have been drilled in the field and range between 600-2750 m depth (LaGeo, 2017b). The average elevation of the wells is about 800 m a.s.l. and the separation pressure of the wells is typically between 6 and 7 bar-a (Jacobo, 2003; LaGeo, 2017a).

The Ahuachapán geothermal field power plant has an installed capacity of 95 MWe and 80 MWe of electricity have been produced with 19 production wells (LaGeo, 2017b). Wells are operating with an average measured enthalpy of 1240 kJ/kg. The electrical power potential produced by individual wells varies between 2.6 and 7.4 MW (Montalvo, 1994; Quijano 1994; LaGeo, 2017a).

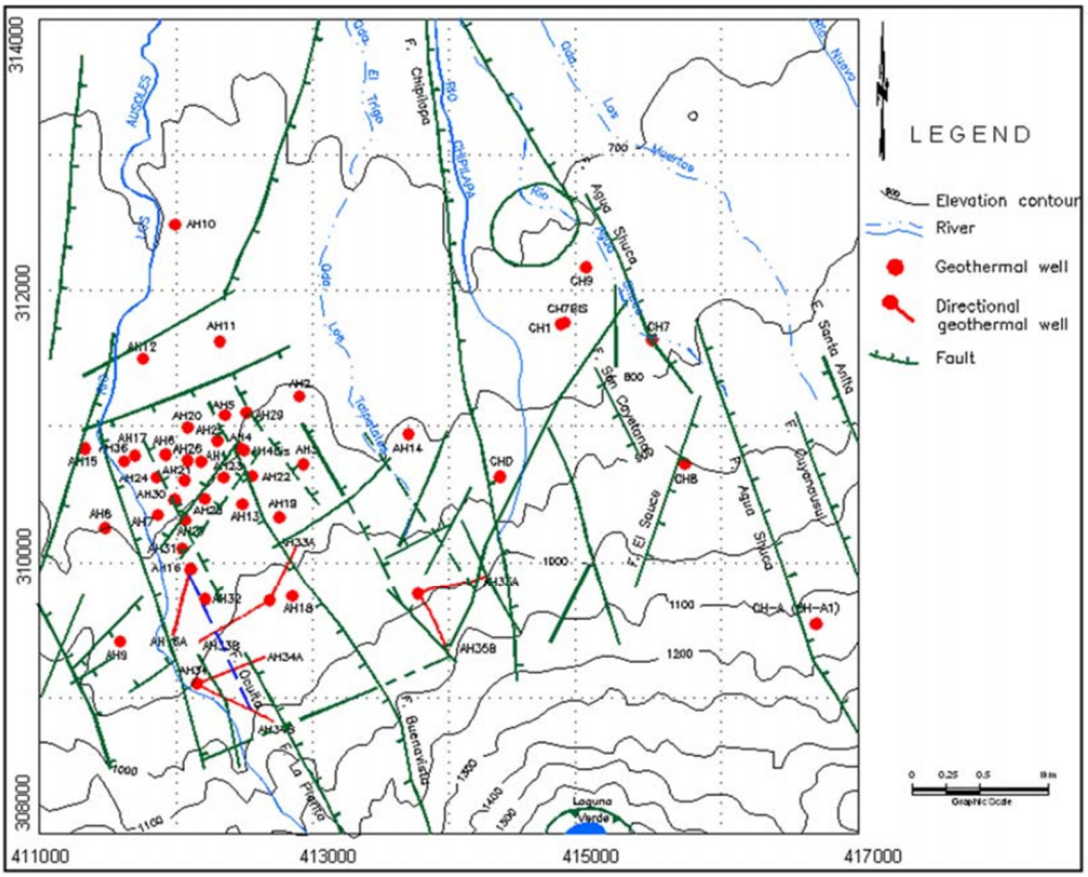

FIGURE 2: Ahuachapán geothermal field system

2.2 Geological setting

El Salvador is situated at the tectonically active margin between the Cocos and Caribbean plates and high temperature geothermal activity in El Salvador is concentrated around the plate subduction zones. The geologic and tectonic processes of both plate margins contribute directly to generating the main engines for geothermal resources: heat and rock permeability (Aunzo et al., 1989; Laky et al 1989; Barrios et al., 2011).

Ahuachapán geothermal field is associated with the south flank of the central Salvadoran median trough and the northwest sector of the Cerro Laguna Verde volcanic group. This extrusive complex developed during Quaternary times near the Pliocene tectonic block of Tacuba-Apaneca (Cuéllar et al., 1981; Aunzo et al., 1989).

Taking into account the information proposed by the lithological logs of the drilled wells in Ahuachapán, four main layers have been defined: Surface materials (40-100°C, thickness up to 500 m); Young agglomerates, a unit which is essentially impermeable and forms the caprock of the geothermal reservoir (100-130°C); Ahuachapán andesite which constitutes the reservoir formation (180-240°C); and older agglomerates (180-240°C, thickness in excess of 400 m) (Figure 3). The last two layers are related to a saline aquifer with a salinity of 22,000 ppm of TDS (Cuéllar et al., 1981; Aunzo et al., 1989).

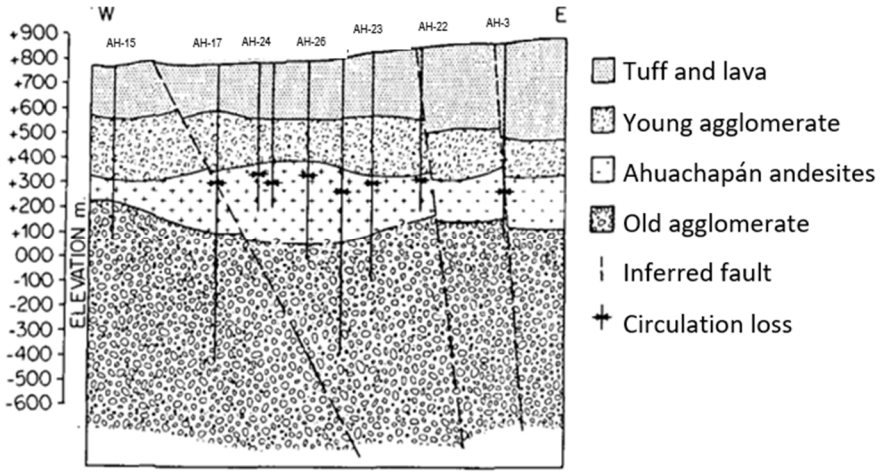

FIGURE 3: Geological cross section of Ahuachapán geothermal field

The surface materials with Holocene rocks (pyroclastics and lavas) contain a shallow aquifer. The aquifer are generally waters of calcium carbonate type with residues below to 500 ppm. The young agglomerates consist of pyroclastics and andesites rocks and contain a regional saturated aquifer. The water of the saturated aquifer is of calcium-sodium carbonate type, with residues below to 400 ppm salinity (Aunzo et al., 1989; Laky et al., 1989; Quijano, 1994).

The regional and local structures are controlled by a system of faults and fractures oriented along three main directions: E-W, which is approximately the trend of the main graben, the most recent system of faults that strike NE-SW, and finally fractures that have a NNW-SSE trend, see Figure 2 (Aunzo et al., 1989; Montalvo, 1994).

2.3 Alteration mineralogy

Chemical exchange occurs during water-rock interaction between hydrothermal fluids and primary minerals, resulting in the hydrothermal alteration of rocks and minerals. This exchange alters the fluid chemistry, dissolves the existing primary minerals and ultimately changes the texture of the rocks (Aunzo et al., 1989).

In the Ahuachapán reservoir, three different alteration zones have been identified:

The shallowest alteration zone, at about 500-780 m depth, is characterized by the presence of chlorite and laumontite. This zone is called phyllic and the formation temperature is in the range of 150-200°C. This unconfined aquifer is recharged by infiltrating rain water and feeds quite a number of springs located on the slopes of the Laguna Verde and Laguna de Las Ninfas volcanoes at the contact with the underlying lavas that constitute the aquiclude and the saline aquifer.

The second alteration zone, called phyllic-prophyllithic, has a depth of 780-1300 m and the predominant minerals are chlorite, wairakite, anhydrite, epidote and illite. The formation temperatures are in the range of 200-250°C.

The third zone is prophyllithic, downwards from about 1300 m. Epidote, anhydrite, wairakite and illite are the minerals present. The formation temperature is in the range of 250-260°C. This zone corresponds to the geothermal reservoir of Ahuachapán field. It has predominantly secondary permeability. Quartz and calcite exist in all three zones (Cuéllar et al., 1981; Aunzo et al., 1989; Laky et al., 1989; Montalvo, 1994: Jacobo, 2003; Montalvo, 2010).

2.4 Composition of the well fluids

The chemistry of the well fluids sampled on the surface show that the fluids are classified as a sodium-chloride type with a chloride range of 3,500-10,000 ppm. They have low Al and Mg concentrations (<1.0 mg/kg), with slightly acid to neutral pH (from 5.5 to 7.9) and the HCO_3 levels vary from 10 to 100 mg/kg. The non-condensable gas content corresponds to around 0.2 to 1.2 % (w/w). CO_2 is the most abundant gas, followed by H_2S.

Results from concentration measurements for metals show low amounts of Pb, Zn, and Cu. They are near or below the limit of quantification for the method (Table 2). Iron shows different behaviour because there are some samples in which the iron concentration is higher. This behaviour may also be due to corrosion of the stainless-steel well casings.

The present study is based on samples collected from wells with a documented history of sulphide-scales. Three wells were selected based on geology reports. One fluid sample was selected per year from 2009 to 2015 for each well (Montalvo, 1994).

3. SCALES IN SURFACE EQUIPMENT

Samples from surface equipment collected during the maintenance breaks of the power plant were separated by macroscopic analysis as metallic and non-metallic and based on color and other physical characteristics. A magnet is mainly used for metallic samples to identify magnetite, which is usually part of the corrosion products (Figure 4).

FIGURE 4: Deposits samples from separators in Well AH-6 and AH-28

Additionally, X-ray diffraction analysis was made to determinate the mineralogy and composition of the samples. Bulk samples and the separated ones were pulverized with an automatic set of mortar and pestle, although for a few samples, pulverization was done manually with an agate mortar and pestle. Samples were run with 2 up to 60° to identify qualitatively the chemical and mineralogical composition, with the help of the EVA software (Diffracplus program).

Most of the minerals reported are chalcopyrite, galena and pyrite as sulphide deposits (Table 1). Most of the minerals have been found in conjunction with other minerals such as quartz and some oxide deposits, e.g. magnetite and hematite (LaGeo, 2008; LaGeo, 2015).

The concentration of metal sulphides in the scale varies from 100% to 8%. The highest metal sulphides concentrations are those of chalcopyrite scales formed on the separator of well AH-23.

TABLE 1: Mineralogy of the scale samples from wells in Ahuachapán Geothermal Field

Well name:	AH-4BIS	AH-19	AH-21	AH-22	AH-23	AH-26	AH-27	AH-31
Chalcopyrite ($CuFeS_2$)	x	x	x	x	x	x	x	x
Sphalerite (ZnS)	x	x	x	x				x
Galena (PbS)	x	x	x	x				x
Pyrite(FeS_2)	x		x		x	x	x	x
Bornite (Cu_5FeS_4)	x						x	
Pyrrhotite ($Fe_{1-X}S$)			x		x	x		
Digenite (CuS)	x		x				x	
Mackinawite(FeS)	x		x				x	
Covellite (CuS)								
Alabandite (MnS)		x						
Oxides	x	x	x	x	x	x	x	x
Clay	x		x			x	x	x
Quartz						x	x	x
Calcite		x		x		x		

4. METHODS

4.1 Sampling programme and analyses

The chemistry of the geothermal fluid is an important factor in the utilization of geothermal resources. Chemical analysis can provide valuable information about the variations that arise during utilization. The collection of water and steam samples from the wells is a routine task.

The method of sample collection and sample preservation until they are analysed depends on which elements will be analysed. Different preservation methods exist for the several processes. Preservation methods can be physical and chemical. The collection of representative samples is important for a good prediction based on the chemical results of the collected samples (Arnórsson et al., 2006).

Continuous annual geochemical monitoring of fluids from production and reinjection wells has been conducted since 1994 in the Ahuachapán geothermal field. Usually samples are collected every three months, but in some cases, as for the wells with calcite scales, samples are collected monthly.

For production wells, steam and water samples are collected at the same pressure using a Webre separator. Steam samples are collected in duplicate into evacuated gas sampling bulbs containing 50 mL of a 4 M NaOH solution. Water samples are collected and split in portions. The samples are preserved physically or chemically, depending on the component to be analysed, and the analytical methods employed.

Chemical analyses are performed at the central geochemical laboratory of LaGeo, which is an accredited laboratory. Table 2 shows the general sample preservation and method of analysis for two-phase geothermal wells.

TABLE 2: Sample treatment and analysis method of geothermal fluids in the LaGeo geochemical lab

Phase	Element	Treatment	Analytical method
Liquid	Na	Filtered/ filter membrane pore size 0.45 µm, 1 mL concentrate HNO_3 (High purity)	AAS
	K	Filtered/ filter membrane pore size 0.45 µm, 1 mL concentrate HNO_3 (High purity)	AAS
	Ca	Filtered/ filter membrane pore size 0.45 µm, 1 mL concentrate HNO_3 (High purity)	AAS
	Mg	Filtered/ filter membrane pore size 0.45 µm, 1 mL concentrate HNO_3 (High purity)	AAS
	B	Filtered/ filter membrane pore size 0.45 µm, 1 mL concentrate HNO_3 (High purity)	AAS
	Al	Filtered/ filter membrane pore size 0.45 µm, 1 mL concentrate HNO_3 (High purity)	ICP/AAS
	Fe	Filtered/ filter membrane pore size 0.45 µm, 1 mL concentrate HNO_3 (High purity)	ICP/AAS
	Cu	Filtered/ filter membrane pore size 0.45 µm, 1 mL concentrate HNO_3 (High purity)	ICP/AAS
	Pb	Filtered/ filter membrane pore size 0.45 µm, 1 mL concentrate HNO_3 (High purity)	ICP/AAS
	Zn	Filtered/ filter membrane pore size 0.45 µm, 1 mL concentrate HNO_3 (High purity)	ICP/AAS
	As	Filtered/ filter membrane pore size 0.45 µm, 1 mL concentrate HNO_3 (High purity)	ICP/AAS
	SiO_2	Dilution/ 10 mL of sample added to 90 mL of deionized water	AAS
	Cl	Filtered/ filter membrane pore size 0.45 µm	Titration with $AgNO_3$
	SO_4	Filtered/ filter membrane pore size 0.45 µm	UVS
	F	Filtered/ filter membrane pore size 0.45 µm	ISE
	EC	Filtered/ filter membrane pore size 0.45 µm	Potentiometric
	NH_3	Acidification/0.5 mL of concentrated H_2SO_4	ISE
	HCO_3	Unfiltered/ completed filled bottle, air free	Titration with HCl and NaOH
	pH	Unfiltered/ completed filled bottle, air free	Potentiometric
	Isotopes	None	Mass Spectrometry
Steam	NH_3	Evacuated double port gas bottle containing 50 mL of 2 M H_3BO_3	ISE
	Isotopes	None	Mass Spectrometry
	CO_2	Evacuated single stopcock valve gas bottle containing 50 mL of 4 M NaOH	Titration with HCl
	H_2S	Evacuated single stopcock valve gas bottle containing 50 mL of 4 M NaOH	Titration with sodium thiosulphate
	H_2	Evacuated single stopcock valve gas bottle containing 50 mL of 4 M NaOH	GC
	He	Evacuated single stopcock valve gas bottle containing 50 mL of 4 M NaOH	GC
	CH_4	Evacuated single stopcock valve gas bottle containing 50 mL of 4 M NaOH	GC
	Ar	Evacuated single stopcock valve gas bottle containing 50 mL of 4 M NaOH	GC
	N_2	Evacuated single stopcock valve gas bottle containing 50 mL of 4 M NaOH	GC
	O_2	Evacuated single stopcock valve gas bottle containing 50 mL of 4 M NaOH	GC

AAS = Atomic Absorption Spectrophotometer ISE = Ion Selective Electrode
UVS = Ultra Violet Spectrophotometer ICP = Inductively Coupled Plasma
GC = Gas Chromatography

4.2 Reservoir fluid composition

Sampling conditions are different between wells and chemical analytical results cannot be compared directly. Therefore, surface chemical data is used for the reconstruction of the fluid at reservoir conditions.

The first step in the geochemical modelling of the geothermal system is the calculation of deep reservoir characteristics from the measured physical-chemical parameters at surface. Chemical concentrations are converted to the reservoir conditions by using chemical geothermometers and equations for the conservation of mass and energy. The reconstruction of the fluid is done in order to predict the state of the water-rock interaction and reservoir processes.

The computer programs for chemical modelling of the equilibrium state of multi-component fluids are useful tools for understanding the behaviour of water chemistry in nature and tracing the reaction mechanisms and processes (Verma, 2012).

The reservoir fluid composition was calculated from the samples of two-phases discharges collected at surface. The WATCH speciation program version 2.4, (Arnórsson et al., 1982; Bjarnason, 2010) was used to calculate the component concentrations in the geothermal reservoir. The input to the program is the component analysis of water, gas and steam condensate of samples collected at surface, including the water pH and temperature at which it was measured.

In the calculations of the reservoir fluid composition, the program assumes conservation of enthalpy and mass, meaning that no transfer of heat and mass occurs on the way from the reservoir to the surface. Such a system is called isolated (Arnórsson et al., 2007).

The output from the program lists the components and species concentrations as well as the activity coefficients at the reference temperature. Geothermometer temperatures, partial pressures of gases, redox potentials, ionic balance and ionic strength are also calculated. Ion activity products and solubility products of selected minerals are computed, this data is useful for calculating mineral saturation indices. However, many metal sulphides under examination in this study are excluded from the WATCH database.

Three wells with different reservoir temperatures were selected for the reconstruction at reservoir conditions. For each of the wells, the data series for the years 2014 and 2015 were processed. The selected reference temperatures used for the calculations were based on downhole measurements and ranged from 208 to 228°C. The samples were collected at pressures between 3.5 and 7.0 bar-g.

After calculating the reservoir fluid composition, WATCH was also used to calculate the composition of the liquid and gas phases, as well as the steam fraction during stepwise adiabatic boiling from the reservoir temperature to the sampling temperature.

4.3 Aqueous speciation and mineral saturation

Aqueous speciation and mineral saturation were calculated with the aid of the SOLMINEQ.88 program, with a particular focus on changes in the saturation index of selected minerals with temperature. This was done both for the calculated reservoir fluid and for the boiled liquid phase at each step.

SOLMINEQ.88 computes the equilibrium distribution of 340 inorganic and organic aqueous species of major, minor and trace elements present in waters. The distribution of aqueous species for a given composition of water at a specified pH and temperature is computed by solving a set of mass-action, oxidation-reduction and mass balance equations based on the ion-association aqueous model.

The saturation state of a mineral in a given solution represents its equilibrium or non-equilibrium with that solution. It can be used to predict whether a given mineral is stable, forming or dissolving in the water. The mineral saturation index (SI) is defined as the logarithm of the ratio of the reaction quotient (Q), equal to the ion activity product (IAP), and the equilibrium constant (K), at the specified temperature and pressure:

$$SI = \log (Q/K) \quad (1)$$

At equilibrium, SI is equal to zero, whereas if SI is below zero, the fluid is under-saturated with respect to the mineral and the mineral (if present) will dissolve into the aqueous phase. If SI is above zero, the fluid is super-saturated and the mineral may precipitate.

In SOLMINEQ.88, two SIs are used to test for possible dissolution or precipitation of minerals. The program computes the Gibbs free energy difference (ΔG diff) between the actual and equilibrium states of the mineral in a given deep liquid, as well as the saturation index given by equation (1).

$$\Delta G \text{ diff} = -RT\ln K - (-RT\ln Q) = RT\ln (Q/K) \quad (2)$$

Here R is the gas constant, T is temperature in degrees Kelvin, Q is the reaction quotient and K is the equilibrium constant. The sulphide mineral reactions used in SOLMINEQ.88 considered in the study are shown in Table 3 (Kharaka et al., 1988).

At equilibrium, Q-K and ΔG diff ‹0. In this case, the subsurface water is in equilibrium with the mineral and no dissolution or precipitation should take place.

TABLE 3: Dissolution reactions for sulphide minerals used in the SOLMINEQ.88 program

Mineral	Reaction
Bornite	$Cu_5FeS_4 + 4H^+ \leftrightarrow 4Cu^+ + Cu^{2+} + Fe^{2+} + 4HS^-$
Chalcocite	$Cu_2S + H^+ \leftrightarrow 2Cu^+ + HS^{--}$
Chalcopyrite	$CuFeS_2 + 2H^+ \leftrightarrow Cu^{2+} + Fe^{2+} + 2HS^-$
Covellite	$CuS + H^+ \leftrightarrow Cu^{2+} + HS^-$
Galena	$PbS + H^+ \leftrightarrow Pb^{2+} + HS^-$
Greigite	$Fe_3S_4 + 4H^+ \leftrightarrow 2Fe^{3+} + Fe^{2+} + 4HS^-$
Pyrite	$FeS_2 + H_2O \leftrightarrow Fe^{2+} + 1.75HS^- + 0.25SO_4^{2-} + 0.25H^+$
Pyrrhotite	$FeS + H^+ \leftrightarrow Fe^{2+} + HS^-$
Sphalerite	$ZnS + H^+ \leftrightarrow Zn^{2+} + HS^-$

4.4 Boiling and cooling process

One of the main processes that alter the composition of the reservoir liquid is the boiling process during ascent to the surface. During the boiling process, temperature is reduced as pressure drops. The concentration of gas in an aqueous fluid affects its boiling point. A steam phase begins to form when the sum of the water vapour pressure and the partial pressures of all the dissolved gases becomes equal to the hydrostatic pressure.

Most of the gases initially present in the deep aquifer will be partitioned into the steam phase. As dissolved CO_2 and H_2S are weak acids their transfer into the steam phase causes an increase in the pH of the water phase. On the other hand, non-volatile elements like chloride in the water phase are gradually concentrated due to steam loss. These changes, and the cooling of the fluid by depressurization boiling, produce complicated changes in individual aqueous species activities. This may lead to chemical reactions. For example, H_2S can be oxidized or precipitated as metal sulphides, resulting in a loss of metals from the solution, and CO_2 is transferred into bicarbonate and can precipitate to some extent as calcium carbonate (Arnórsson et al., 2007).

Aqueous speciation and the state of mineral saturation were calculated using SOLMINEQ.88, both for the reservoir aquifer fluids and during boiling and cooling, based on the component concentrations obtained from the WATCH program at each temperature.

5. RESULTS

5.1 Deep fluid composition

The aquifer composition calculated with the help of the WATCH program is given in Table 4. The selected reference temperatures chosen for the calculations were based on downhole measurements. For wells AH-4BIS, AH-19 and AH-23 the reservoir temperatures specified are 208°C, 212°C and 228°C, respectively. The calculated reservoir pH ranged from 4.8 to 5.6, which is close to neutral at those temperatures.

TABLE 4: Calculated reservoir fluid composition from Ahuachapán wells

	AH-4 BIS		**AH-19**		**AH-23**	
	2014	**2015**	**2014**	**2015**	**2014**	**2015**
	(mg/kg)	**(mg/kg)**	**(mg/kg)**	**(mg/kg)**	**(mg/kg)**	**(mg/kg)**
pH	5.00	5.06	5.59	5.61	4.81	4.84
B	90.19	90.95	77.88	68.10	86.41	63.85
SiO_2	387.6	409.3	365.8	371.1	359.7	384.9
Na	3083	3059	2909	2904	2968	3096
K	390.2	391.5	329.0	351.9	388.8	394.6
Mg	0.033	0.042	0.038	0.039	0.022	0.035
Ca	212.5	198.0	182.0	190.3	169.3	160.5
Cl	5516	5343	5055	4917	5146	5251
SO_4	31.34	38.61	32.20	35.27	37.82	40.08
Al	0.086	0.091	0.123	0.171	0.087	0.129
Fe	0.046	0.262	0.071	0.030	0.126	0.197
Cu	0.001	0.001	0.001	0.001	0.001	0.001
Zn	0.001	0.009	0.138	0.001	0.002	0.002
Pb	0.006	0.006	0.005	0.006	0.005	0.006
CO_2	978.9	750.4	382.3	336.4	1801	1601
H_2S	17.00	16.39	14.89	19.92	27.75	25.06
NH_3	0.100	0.100	0.120	0.120	0.110	0.110
H_2	0.160	0.160	0.180	0.180	0.210	0.180
O_2	0.000	0.000	0.000	0.000	0.000	0.000
CH_4	0.290	0.290	0.330	0.340	0.420	0.400
N_2	11.48	12.34	9.32	9.27	26.86	22.36

Well AH-4BIS and well AH-23 are very similar with respect to major non-volatile elements such as Cl, Na, Si, K and B, however, they are different with respect to the concentration of volatiles in the reservoir fluid composition. CO_2 and H_2S are higher in well AH-23 but enthalpy is similar in both wells. In well AH-19, the Cl concentration in the reservoir is slightly lower than in wells AH-4BIS and AH-23, but there is a big difference in the concentration of CO_2. The three wells have similar metal concentrations, which are in the order of ppb. In the chemical history of these wells, a small decrease in the concentration of chlorides has been seen with time. The same behaviour has been observed in the Chipilapa geothermal field which is the reinjection area of the system, and in El Salitre hot spring which is one of the principal manifestations in the area. The changes in well AH-23 suggested boiling during flow to the well and changes in well AH-19 indicated the mixing of cooler, more diluted water according to Montalvo (1994).

5.2 Boiling calculations and aqueous speciation

For the present study, a ten step boiling process was calculated with the aid of the WATCH program. The temperature range used starts at the reservoir temperature and ends at the sample temperature.

Changes in water composition and temperature will cause changes in the state of saturation of the water with respect to minerals. During boiling, the water composition changes in response to steam formation and degassing. Figure 5 shows the relation between temperature and steam fraction during the boiling process in wells AH-4BIS, AH-19 and AH-23. The consequence of these changes is the potential of precipitation or dissolution of the minerals, whose magnitude depends on the kinetic factor (Arnórsson and Gudmundsson, 2003).

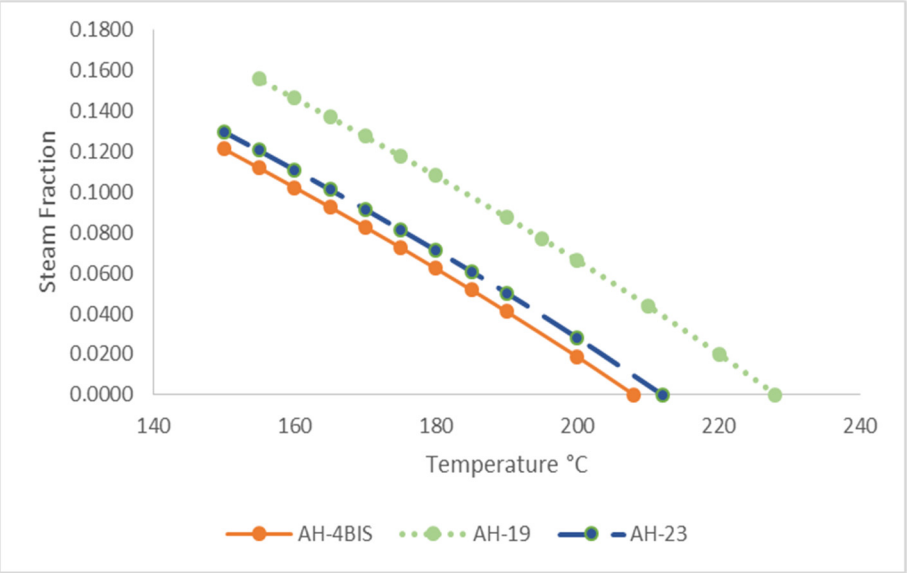

FIGURE 5: Relationship between temperature and steam fraction during the boiling process

Figure 6 shows how pH increases when temperature decreases. Volatile gases such as CO_2, H_2S, and NH_3 break off due to the formation of the steam phase. The loss of these gases may drastically change the pH of the remaining fluids.

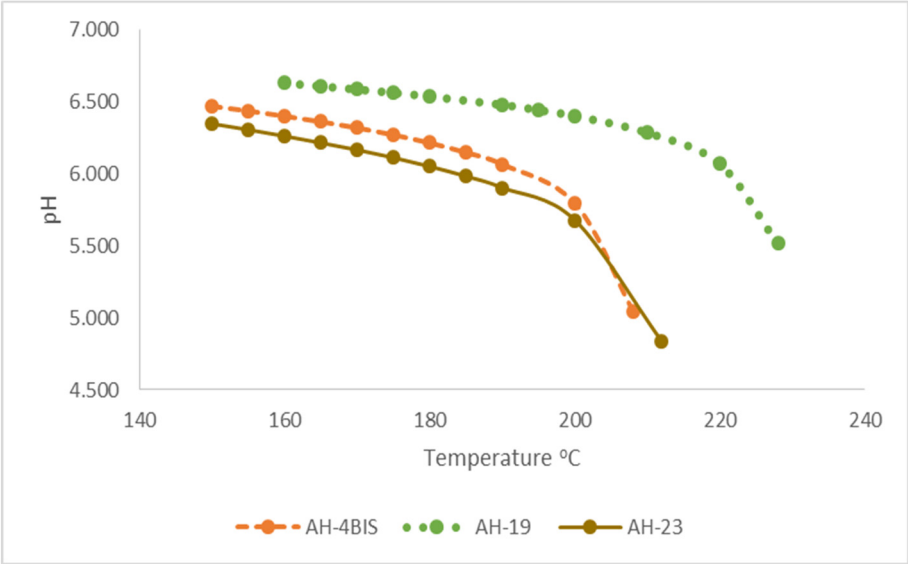

FIGURE 6: Changes in pH value as an effect of boiling

Therefore, the concentrations of volatile gases in the liquid phase decrease when the temperature decreases. Figures 7 and 8 show how the CO_2 and H_2S concentrations decrease in the liquid phase.

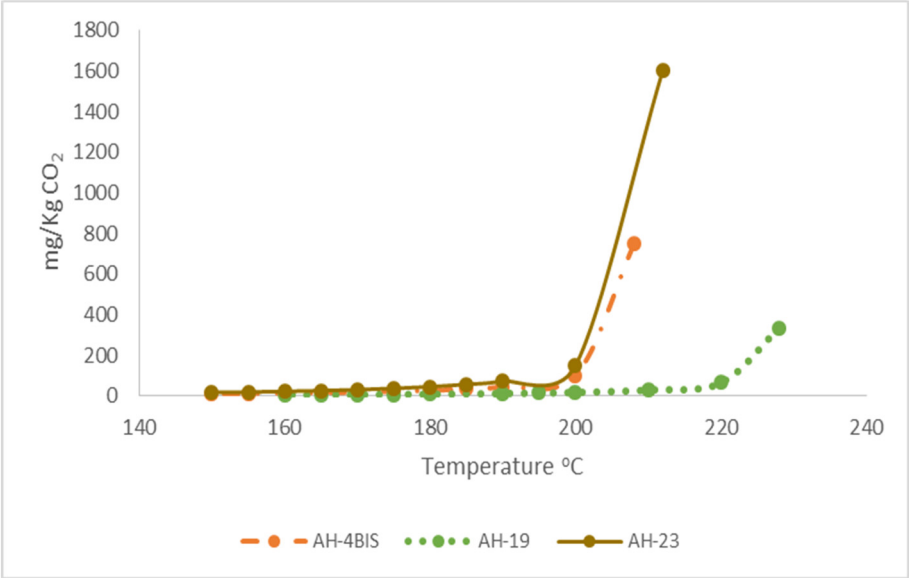

FIGURE 7: Relationship between CO_2 in the liquid phase and temperature during the boiling process

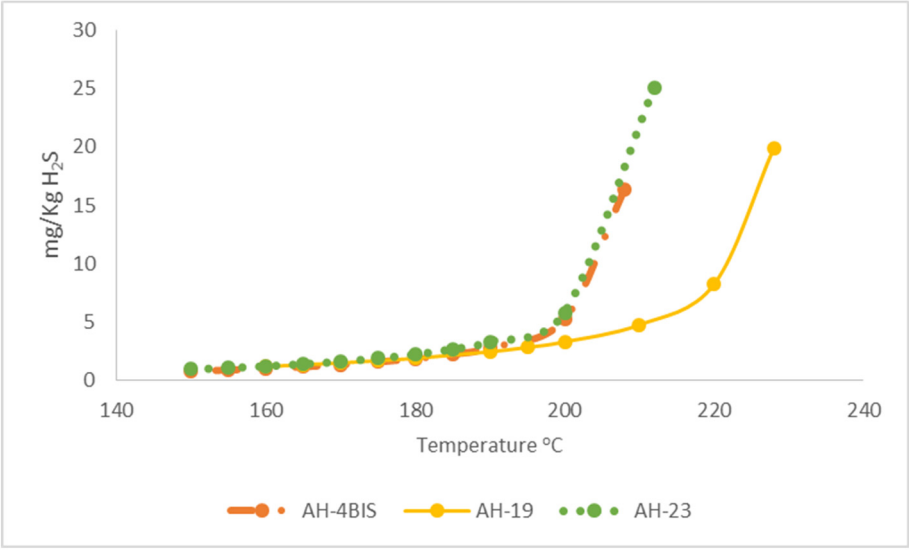

FIGURE 8: Relationship between H_2S in the liquid phase and temperature during the boiling process

On the other hand, non-volatile component concentrations increase when the temperature decreases due to the mass of water loss into the steam phase. Figures 9 and 10 show the behaviour of non-volatile elements when the fluid temperature decreases during boiling. We can see a linear relationship between the concentration of non-volatile elements and temperature.

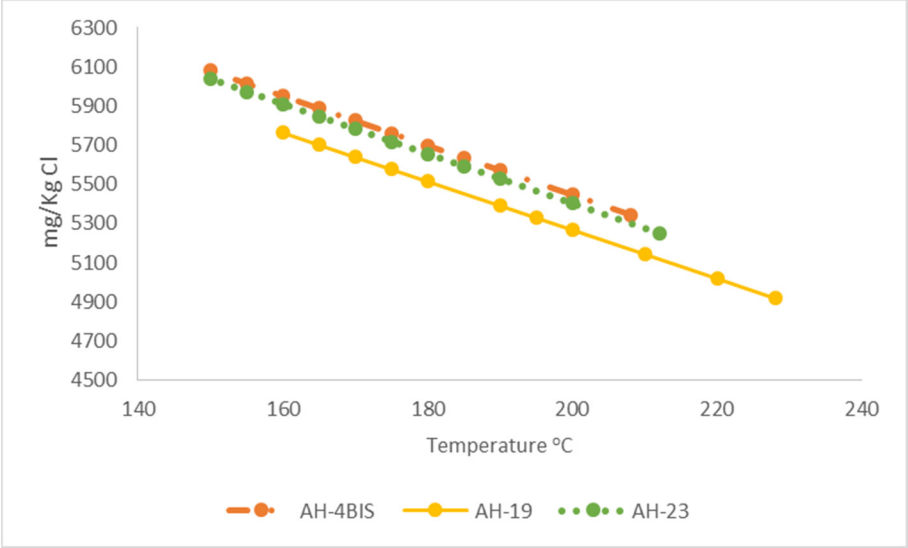

FIGURE 9: Relationship between Cl^- and temperature during the boiling process

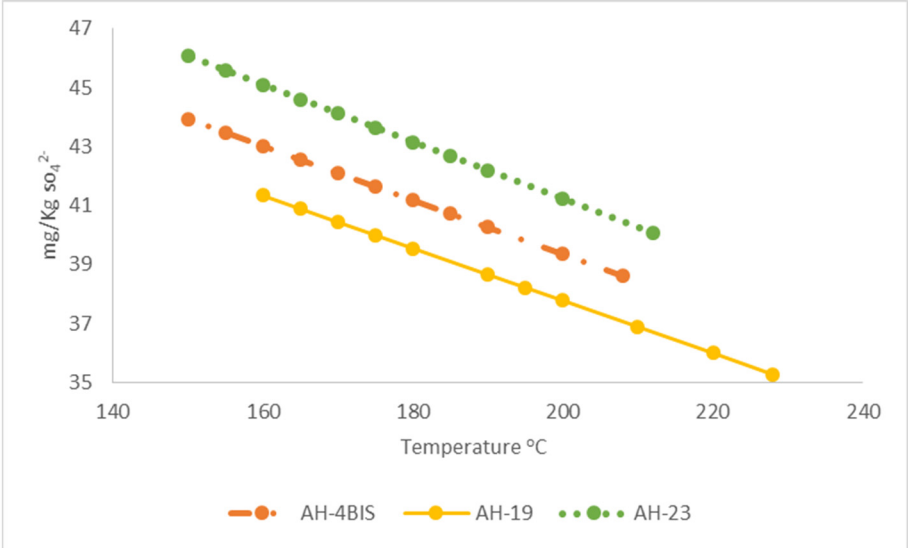

FIGURE 10: Relationship between $SO4^{-2}$ and temperature during the boiling process

Because of these processes of increasing the pH and losing of volatile gases from the water phase, the aqueous species activities change. Cooling and degassing tend to produce water that is over-saturated with respect to minerals whose solubility decreases when the pH increases (Arnórsson et al., 2007).

The distribution of a dissolved component into individual aqueous species concentration is controlled by the equilibrium constant (K), for the dissociation of the species, this means that the aqueous species concentration depends on temperature. The effective concentration of an ion in a solution, after considering the aqueous complex formation, is called ion activity,

$$a_i = m_i \cdot \gamma_i \tag{3}$$

where a_i, is the activity of species i, m_i is the molal concentration of species i, and γ_i is the activity coefficient of species i.

For relatively dilute aqueous solutions, we can calculate γ_i using the Debye-Hückel equation:

$$\log \gamma_i = -Az_i^2 \frac{\sqrt{I}}{1 + B\text{å}\sqrt{I}} \quad (4)$$

where z_i is the charge of species i, I is the ionic strength of the solution, A and B are empirically fitted parameters for a specified temperature, and å is the radius of the hydrated ion (Kharaka et al., 1988).

Geochemical equilibrium programs such as WATCH and SOLMINEQ.88 compute activities of species for some given component concentration, at specified conditions of temperature and pressure.

Due to the effect of the increased pH (H^+ activity decreases), sulphide (S^{2-}) is liberated from H_2S or HS^-. As a result, sulphide minerals can precipitate (Reed and Palandri, 2006; Padilla, 2011).

Figure 11 shows how the activity of H^+ is decreasing when the temperature decreases, and H_2S shows the same behaviour as H^+. However, for HS^- and S^{2-}, while the temperature is decreasing the activities of those species rise. The effect of increasing pH (decreasing acitivity of H^+) and increasing activity of HS^- moves the precipitation reaction to the left side, helping to precipitate sulphides (see Table 3).

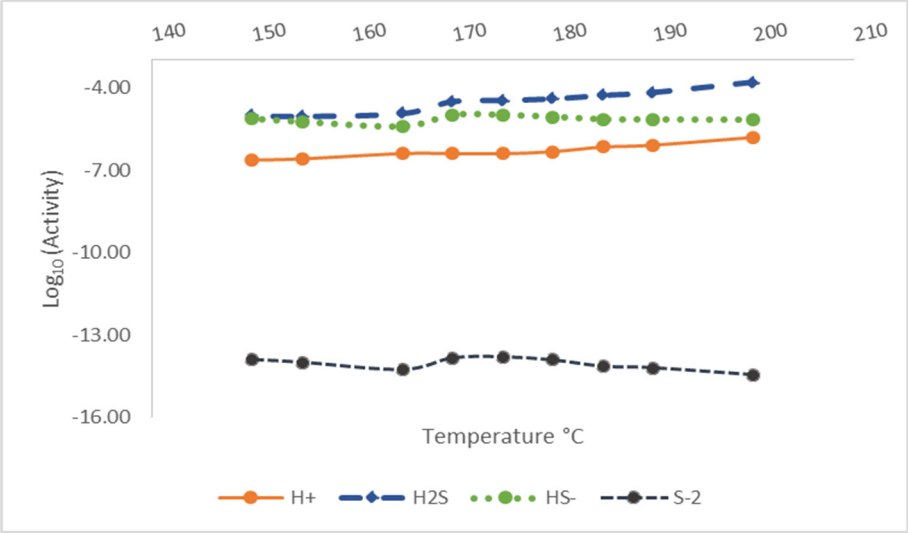

FIGURE 11: Logarithm of the activities of component species in the boiling process, as follows: H^+, H_2S, HS^-, S^2

Reed and Palandri (2006) showed that Cl^- complexes compete with the HS^- complex to bind metals, so we can say that the Cl^- concentration affects the formation of metal sulphides. As chloride species of Pb^{2+}, Zn^{2+} and Fe^{2+} are more stable at high temperatures than at low ones, which means that when temperatures decrease with boiling, more of the free metal ions become available for precipitation as sulphides. For example, the Cu-Cl complex has a dissociation peak at 200°C suggesting that at lower temperatures, sulphide minerals are more likely to precipitate.

5.3 Mineral saturation

As mentioned before, the mineral saturation index is defined by the quotient of the ion activity product (Q) of the species that form the mineral and the mineral thermodynamic equilibrium constant (K). Both are temperature dependent. Variations of temperature could transport a secondary mineral from an under-saturated state to a saturated or super-saturated state. Saturation indices were calculated with the aid of SOLMINEQ.88 for the following sulphide minerals: pyrite, bornite, chalcopyrite, chalcocite, covellite, galena, pyrite, pyrrhotite and sphalerite, to evaluate which of those minerals are in equilibrium with the geothermal liquid in the reservoir.

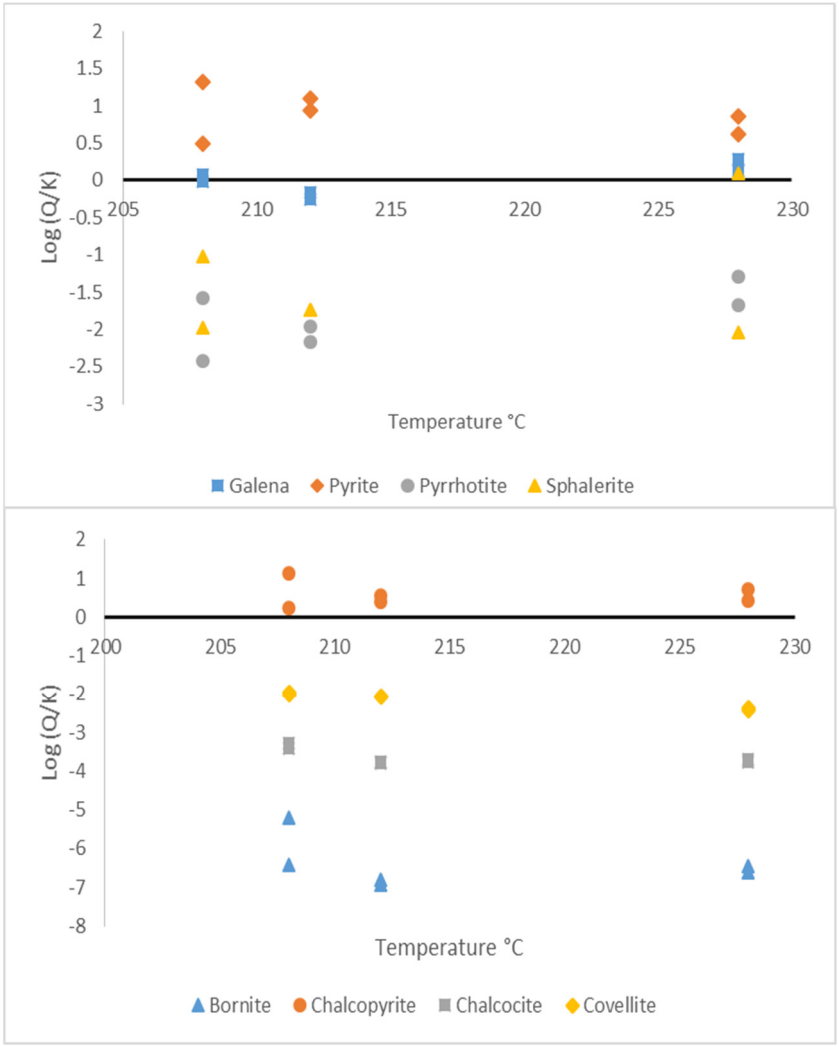

FIGURE 12: Saturation index of sulphide minerals under reservoir conditions

The initial aquifer fluid is predicted to be saturated or super-saturated with chalcopyrite and pyrite in the wells in study. Galena is predicted as saturated in wells AH-4BIS and AH-19. Sphalerite is predicted to be saturated only in one sample from well AH-19. Bornite, chalcocite, pyrrhotite and covellite are predicted to be under-saturated at reservoir conditions in all wells (Figure 12).

Saturation indices were calculated at ten different temperatures, from the reservoir temperature to the separation temperature of each well, simulating boiling and steam loss. Many of the minerals observed in samples are predicted to be super-saturated at the separation temperature, including bornite, chalcopyrite, chalcocite, covellite, galena, and pyrite.

Chalcopyrite and pyrite are saturated at reservoir conditions in all three wells. Galena is saturated at the reservoir temperature only in well AH-19. In both cases, when the temperature is decreasing in the boiling process, the minerals become more super-saturated (Figure 13 and 14).

The fluid composition indicates that the liquids are under-saturated at reservoir conditions with respect to chalcocite, covellite, bornite, pyrrhotite and sphalerite. In the cases of bornite, chalcocite and covellite, they gradually become super-saturated from the initiation of boiling to the separation temperature (Figures 15 and 16), although covellite is only slightly super-saturated. On the other hand, sphalerite and pyrrhotite are under-saturated from the reservoir conditions to the separation temperature in the data collected in the years 2014 and 2015 (Figures 17 and 18).

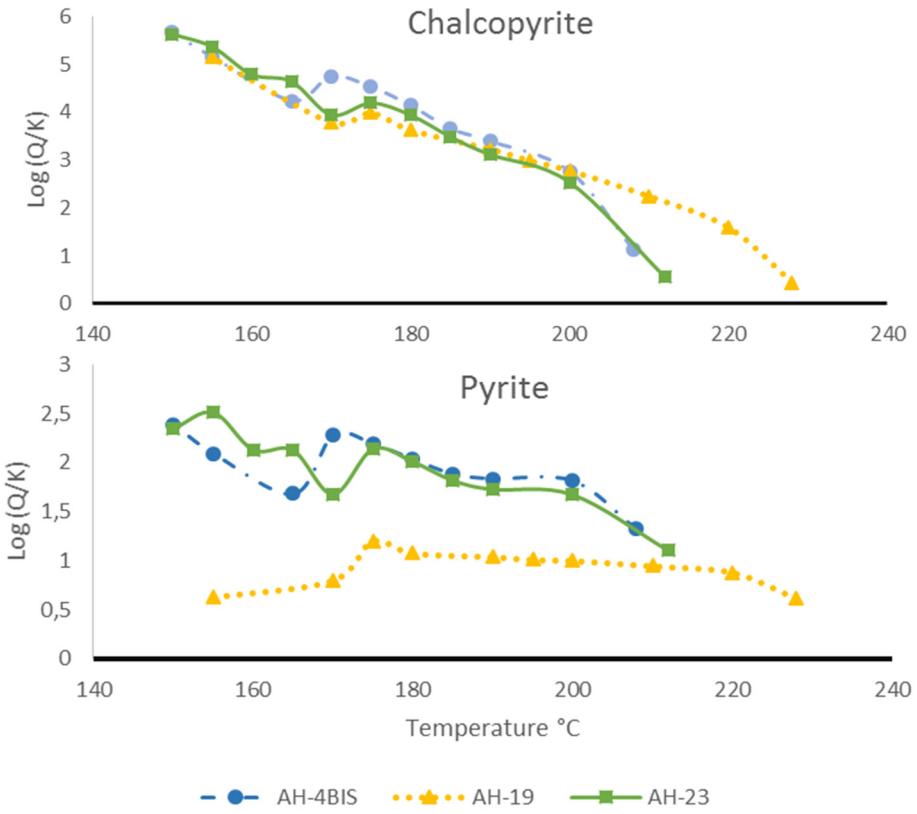

FIGURE 13: Mineral saturation index with respect to chalcopyrite and pyrite, data from 2014

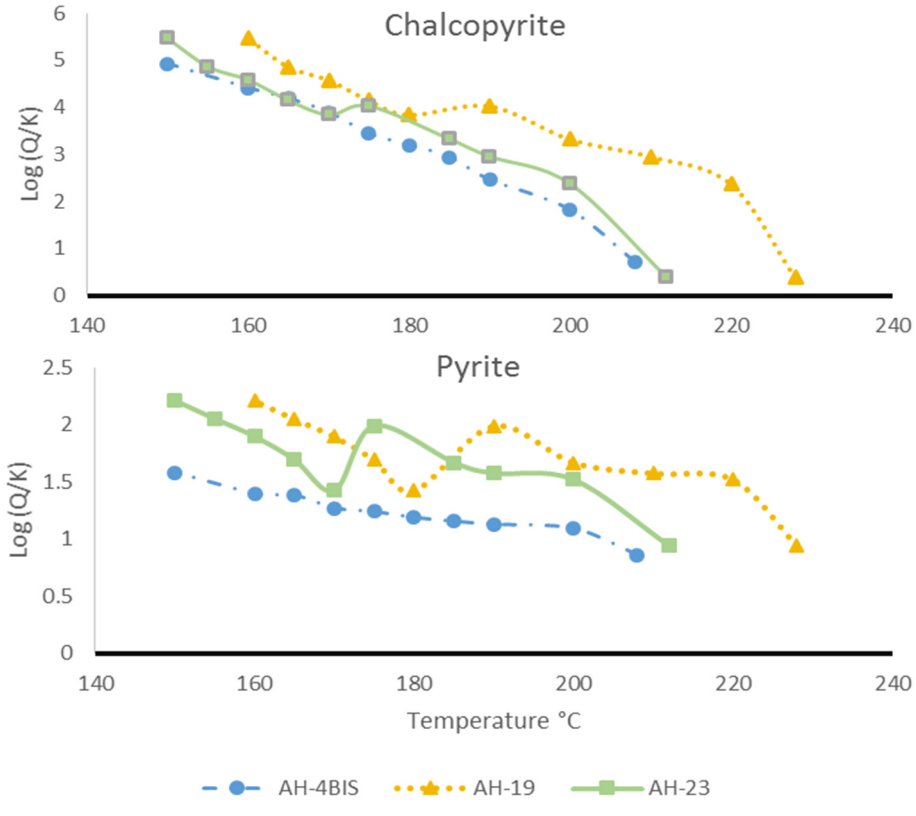

FIGURE 14: Mineral saturation index with respect to chalcopyrite and pyrite, data from 2015

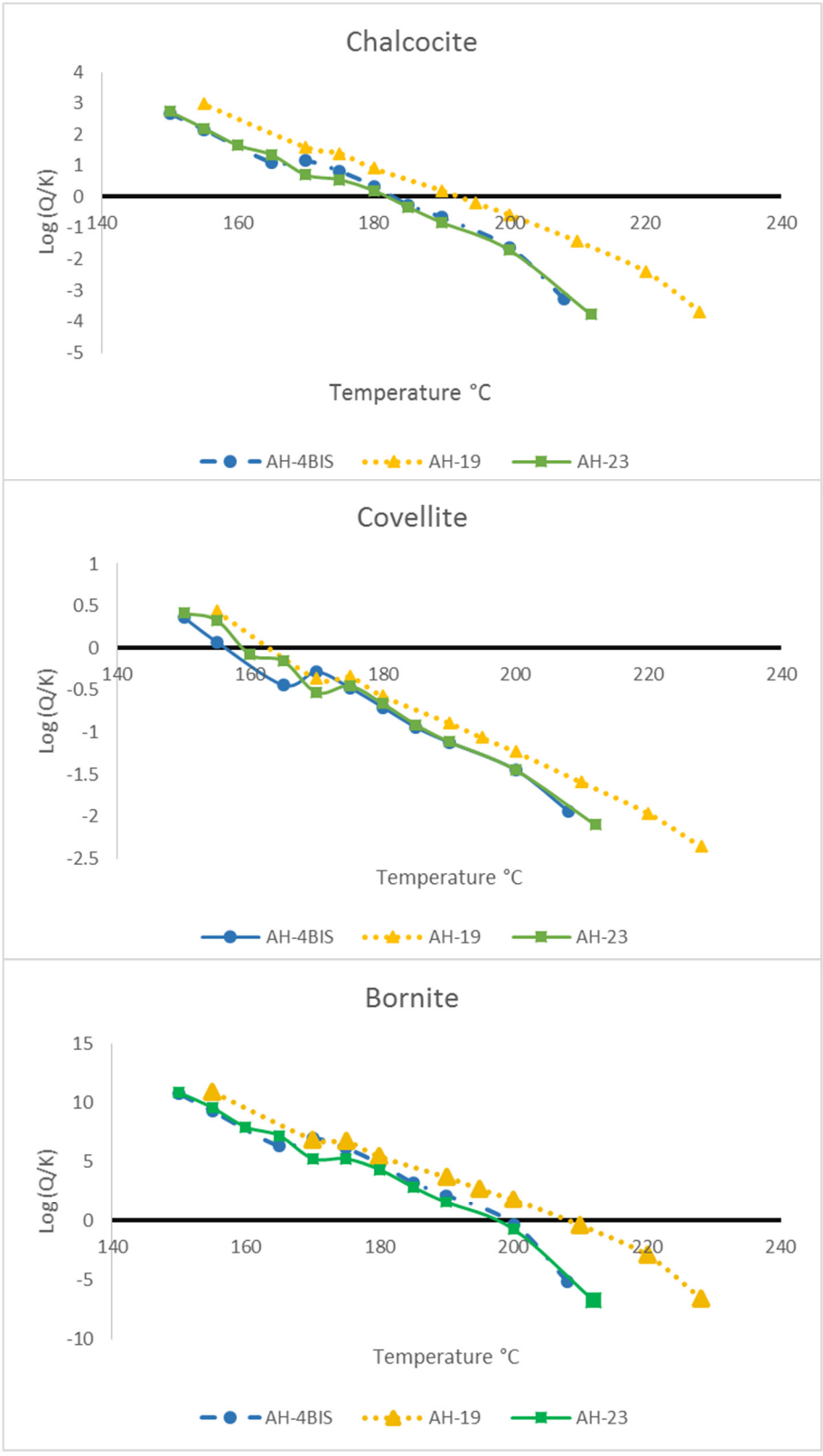

FIGURE 15: Mineral saturation index of chalcocite, covellite and bornite, data from 2014

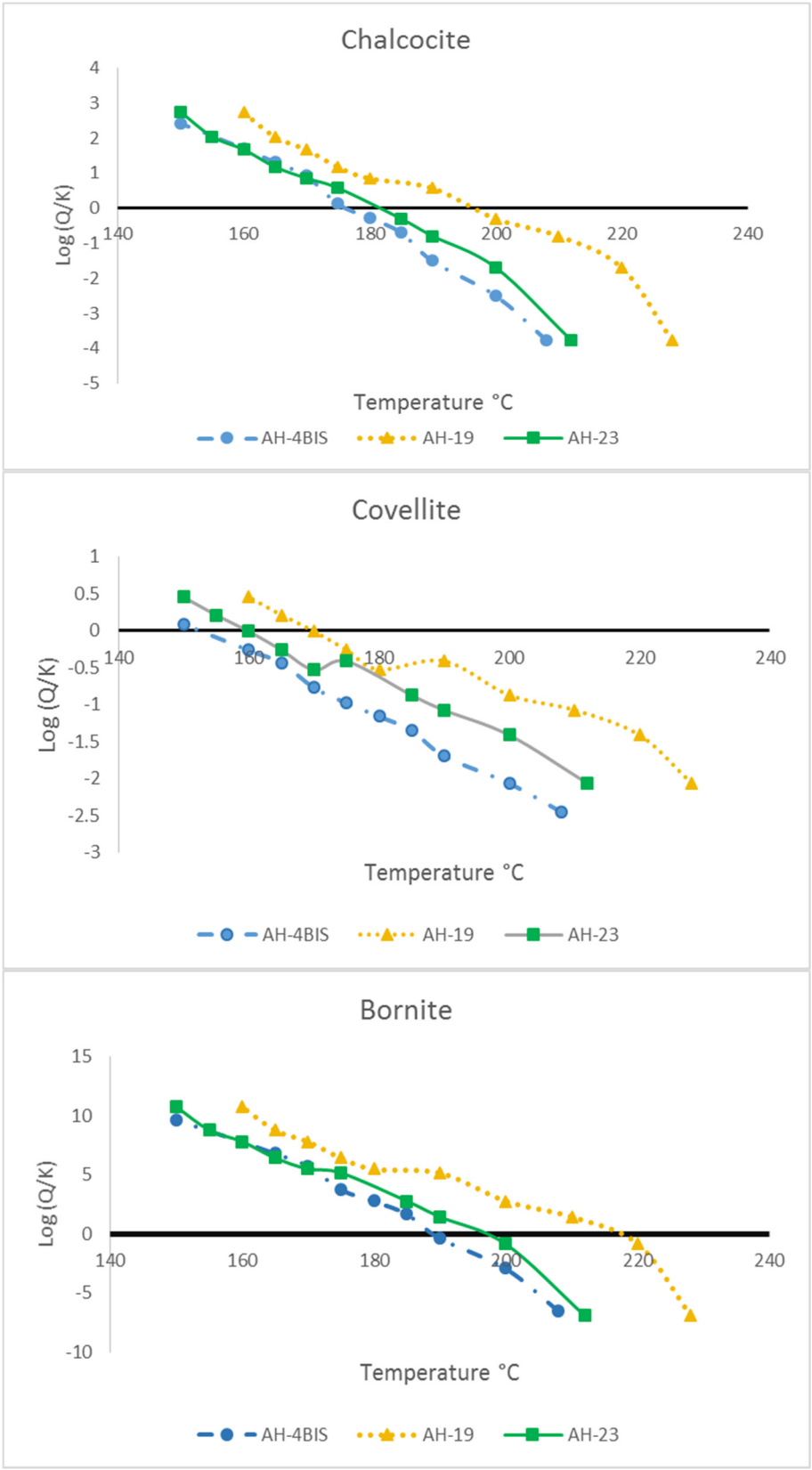

FIGURE 16: Mineral saturation index of chalcocite, covellite and bornite, data from 2015

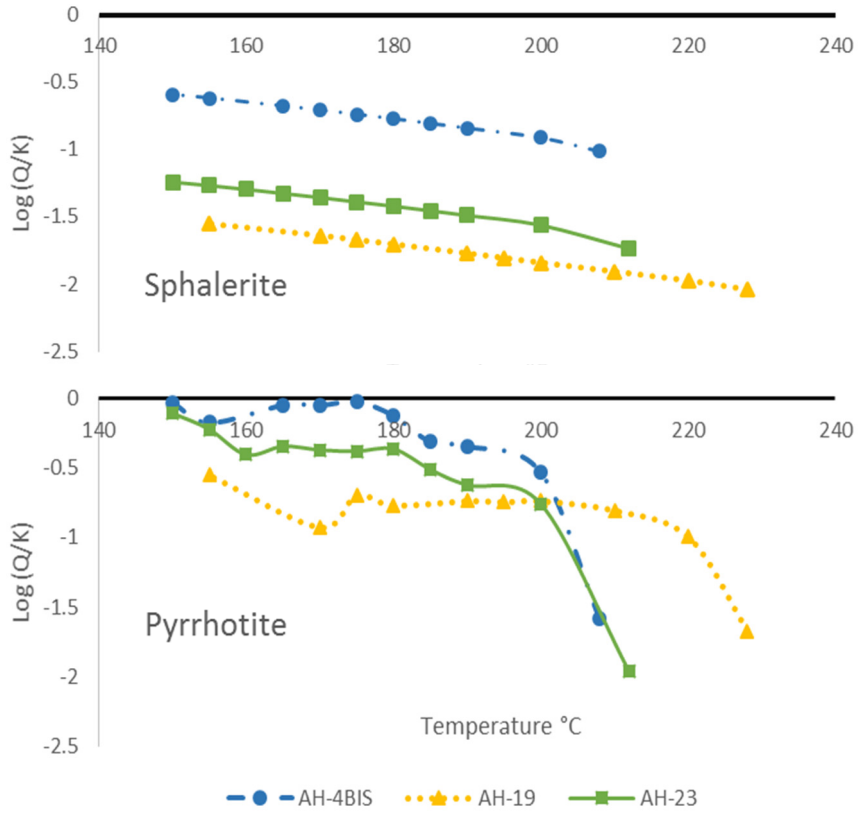

FIGURE 17: Mineral saturation index of sphalerite and pyrrhotite (data from 2014)

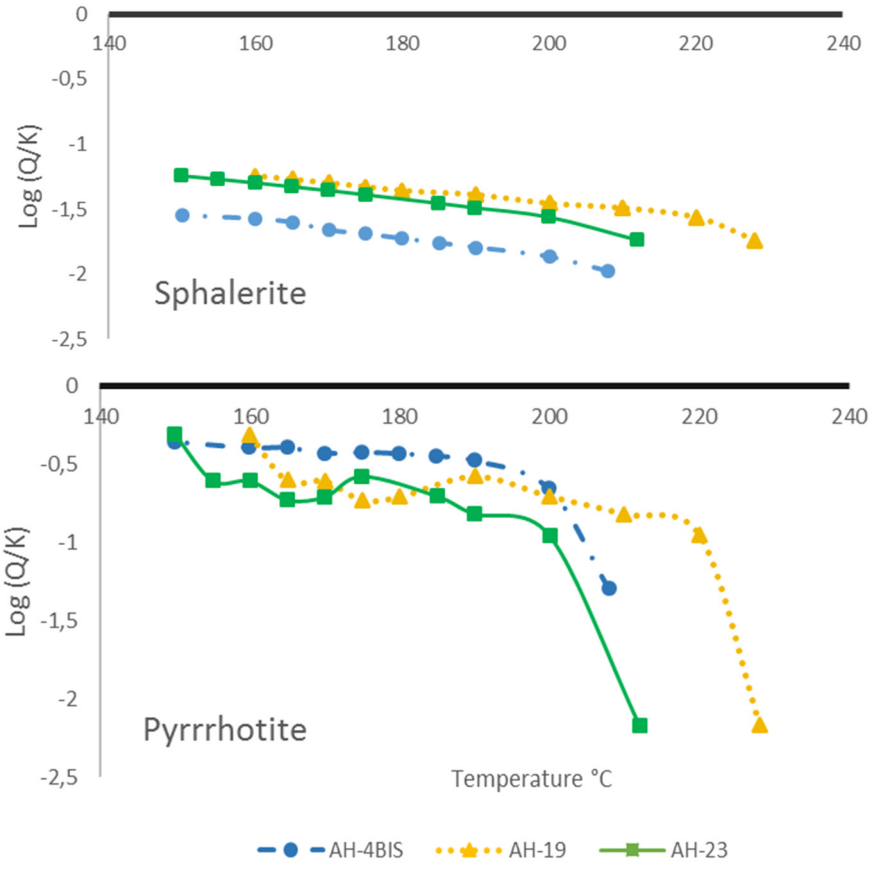

FIGURE 18: Mineral saturation index of sphalerite and pyrrhotite (data from 2015)

Galena is saturated at reservoir conditions in well AH-4BIS in data from both years, and it becomes super-saturated during the boiling process. However, in well AH-19 galena is under-saturated at reservoir conditions only in data from 2014 but in the 2015 data it started as under-saturated and became super saturated in the boiling process. This may be because in the data from 2014 the concentrations of Pb and H_2S are higher than in the data from 2015 at reservoir conditions. In the case of AH-23, galena is under-saturated at reservoir conditions and becomes super-saturated during the boiling process (Figure 19).

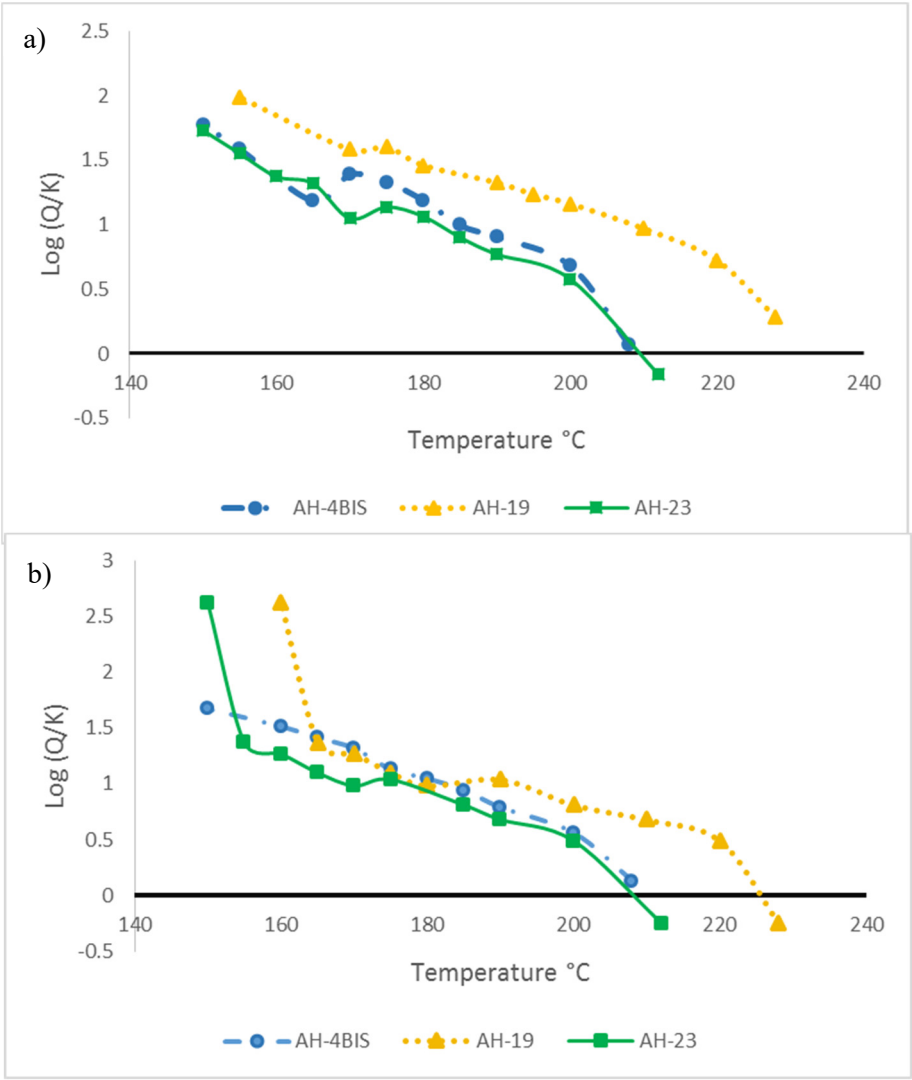

FIGURE 19: Mineral saturation index of galena. Data from 2014 (a) and 2015 (b)

The concentrations of Fe, Cu, Zn and Pb in the fluid discharged at the surface are orders of magnitude lower than in the reservoir fluid in the reservoir fluid due to precipitation and steam loss during the boiling process. Metal concentrations are in magnitudes of ppb. The high metal concentrations in the scales suggest that the metal concentrations in the deep liquid are higher than those sampled on the surface (Hardardóttir et al., 2009).

If we compare the geological results with the chemical modelling predictions, there are some matches. For example, in the geological reports on the scale analysis, pyrite and chalcopyrite are reported in high concentrations in the samples with the exception of well AH-19, where pyrite was not reported in 2014.

If we look at the chemical predictions with respect to these minerals, they are super-saturated from the reservoir conditions and during boiling, they become more super-saturated. The pyrite saturation index in well AH-19 in 2014 has a value of 0.6 at the separation temperature, which is much lower than the value for the same mineral at the same conditions in data from 2015, where it was 2.2.

Galena is observed in trace to moderate quantities in the surface equipment in wells AH-4BIS and AH-19 according to the geological reports, but not in well AH-23. The chemical modelling predicts galena to become super-saturated during the boiling process in all three wells. Sphalerite is also reported in trace concentrations in the geological reports but in the chemical modelling it is predicted to be under-saturated from the reservoir condition and during the entire boiling process.

However, in the cases of chalcocite and covellite, these have not been reported in the geological report but in the chemical modelling these minerals become super-saturated during the boiling process. (although covellite is only slightly super-saturated). This behaviour is observed in all three wells. Bornite appears in the composition of deposits in well AH-4BIS but not in wells AH-19 and AH-23. Nevertheless, the chemical modelling predicts that bornite should become super-saturated during the boiling process.

On the other hand, pyrrhotite is reported by the geological laboratory in a concentration range between 13 and 22%. In the chemical modelling, pyrrhotite is under-saturated both at reservoir conditions and during the boiling process. This may indicate that pyrrhotite is not the result of the chemical reaction in the aquifer but may be the result of secondary process in the formation of a surface reaction product when magnetite reacts with H_2S (Criaud and Fouillac, 1989; Karabelas et al., 1989).

They are many possible sources of errors in the modelling. The most obvious is that the reported concentrations of H_2S and metals are incorrect or do not represent the reservoir fluid, the former being sensitive to oxidation and the latter often in trace concentrations very close to the method detection limits. In the case of Zn, there is also a large difference in surface concentrations between the two data sets, especially for wells AH-19 and AH-4BIS. Another possible source of errors may be in the thermodynamic data used by the speciation programs. The assumption of the metal/H_2S ratio in the fluids, which may change the redox buffers that determine precipitation reactions, may be yet another source of error.

Finally, the calculations presented here are carried out for a static system, i.e. no reaction path modelling was conducted. Therefore, possible effects of reaction kinetics were neglected, and more importantly, no mineral precipitation was simulated. The precipitation of one metal sulphide (e.g. chalcopyrite) at the onset of boiling would change the fluid composition (in particular the concentrations of S^{2-}, Cu and Fe) and thereby lower the calculated saturation indices of the other metal sulphides. This may explain why only some of the mineral phases predicted to precipitate during boiling were actually observed in the scales. It means that some sulphides have already precipitated in the well before the fluid was sampled. This effect has been observed in Reykjanes (Hardardóttir et al., 2009; Hardardóttir, 2011) and in Taupo, New Zealand (Simmons and Brown, 2007). Similar success have been notes for wells with calcite scaling.

6. CONCLUSIONS

At the separation temperature, the fluid in wells AH-4BIS, AH-19 and AH-23 is predicted to be super-saturated with respect to bornite, chalcopyrite, chalcocite, galena, and pyrite. These results are coherent with the results obtained by the geology laboratory. The most important metals for sulphide transport are Fe, Cu and Pb.

The results after the reconstruction of the fluid composition at reservoir conditions indicate that chalcopyrite and pyrite are super-saturated under aquifer conditions in the wells under study and galena is super-saturated only in wells AH-19 and AH-4BIS. However, bornite, covellite, pyrrhotite, and sphalerite are under-saturated. After the temperature begins to decrease and the steam fraction begins to increase (boiling process), sulphide minerals become more super-saturated for those minerals that start to precipitate under aquifer conditions and saturated for those minerals that are under-saturated under aquifer conditions.

Changes of temperature and pH are clearly very important parameters affecting sulphide precipitation in natural systems.

Knowledge of the chemical composition of geothermal waters is vital for predicting the behaviour of the liquid reservoir as well as for the behaviour of the liquid on the way to the surface. However, not only thermodynamics have an important role in this prediction; instrumental chemistry also has a very important role. Careful measurements of water quality and systematic analysis of the data allow the best prediction of the potential problem.

ACKNOWLEDGEMENTS

I would like to express my gratefulness to the United Nations University Geothermal Training Programme, for the opportunity to take part in the six-month course. I am so grateful with the entire UNU-GTP staff: Mr. Lúdvík S. Georgsson, Mr. Ingimar Haraldsson, Ms. Málfrídur Ómarsdóttir, Ms. Thórhildur Ísberg and Mr. Markús A. G. Wilde for their time and help.

I would also like to extend my gratitude to my employer, LaGeo S.A de C.V, for giving me the chance and time to undertake this training. I want to thank my colleagues for their support and help, special appreciations to Kevin, Jeannette, Diana, Elizabeth, Antonio, Jaime, Harold and Angel.

My deepest gratitude to my supervisor Mr. Finnbogi Óskarsson for his guidance, help and sharing of time and knowledge.

Special acknowledgements also go to my loved husband, Héctor, for the moral support, patience, love and prayers during my stay in Iceland. My deepest thanks go to my parents, Alcides and Silvia, for their prayers, guidance and encouragement all my life. Thanks to all my family for their support during these months. Finally, I want to thank God for his blessings during my stay in Iceland.

REFERENCES

Andritsos, N., and Karabelas, A.J., 1991: Sulphide scale formation and control: the case of lead sulphide. *Geothermics, 20*, 343-353.

Andritsos, N., and Karabelas, A.J., 1995: An experimental study of sulphide scale formation in pipes. *Proceedings of the World Geothermal Congress 1995, Florence, Italy, 2469-2474.*

Arnórsson, S., Bjarnason, J.Ö., Giroud, N., Gunnarsson, I., and Stefánsson, A., 2006: Sampling and analysis of geothermal fluids. *Geofluids, 6, 203-216*.

Arnórsson, S., and Gudmundsson, B., 2003: Geochemical monitoring response of geothermal reservoirs to production load – examples from Krafla, Iceland. *Presented at "International Geothermal Conference", Reykjavik, 2003.* 30-36.

Arnórsson, S., Sigurdsson, S. and Svavarsson, H., 1982: The chemistry of geothermal waters in Iceland I. Calculation of aqueous speciation from 0°C to 370°C. *Geochim. Cosmochim. Acta, 46,* 1513-1532.

Arnórsson, S., Stefánsson, A., and Bjarnason, J.Ö., 2007: Fluid-fluid interaction in geothermal systems. *Reviews in Mineralogy & Geochemistry*, *65,* 229-312.

Aunzo, Z., Bödvarsson, G.S., Laky, C., Lippmann, M.J., Steingrímsson, B., Truesdell, A.H. and Witherspoon, P.A., 1989: *The Ahuachapan geothermal field, El Salvador - Reservoir analysis - volume I: text and main figures*. Lawrence Berkeley Laboratory Report, LBL-26612, 216 pp.

Banks, J.C. 2013: *Sulphate mineral scaling during the production of geothermal energy from sedimentary basin formation brine: A case study at the Groß Schönebeck in-situ geothermal laboratory, Germany.* Freien Berlin University, Fachbereich Geowissenschaften, PhD thesis, 149 pp.

Barrios, L., Hernández, B., Quezada, A., and Pullinger, C., 2011: Geological hazards and geotechnical aspects in geothermal areas, the El Salvador experience. *Presented at "Short Course on Geothermal Drilling in Central America – Resource Development and Power Plants", UNU-GTP and LaGeo, Santa Tecla, El Salvador,* 14 pp.

Bjarnason, J.Ö., 1994: *The speciation program WATCH, version 2.1.* Orkustofnun, Reykjavík, 7 pp.

Bjarnason, J.Ö., 2010: *The chemical speciation program WATCH, version 2.4*. ÍSOR – Iceland GeoSurvey, Reykjavik, website: *www.geothermal.is/software.*

Cuéllar, G., Choussy, M., and Escobar, D., 1981: Extraction-reinjection at Ahuachapán geothermal field. In: Rybach, L., and Muffler, L.J.P., (editors), G*eothermal systems. Principles and case histories.* John Wiley and Sons Ltd., Chichester, 321-336.

Criaud, A. and Fouillac, C., 1989: Sulphide scaling in low-enthalpy geothermal environments: a review. *Geothermics, 18*, 73-81

Hardardóttir, V., Brown, K.L., Fridriksson, Th., Hedenquist, J.W., Hannington, M.D., Thorhallsson, S., 2009: Metals in deep liquid of the Reykjanes geothermal system, southwest Iceland: Implications for the composition of seafloor black smoker fluids. *Geology, 37/12*, 1103-1106.

Hardardóttir, V., 2011. *Metal-rich scales in the Reykjanes geothermal system, SW Iceland: sulphide minerals in seawater-dominated hydrothermal environment*. University of Ottawa, PhD thesis. 311 pp.

Jacobo, P., 2003: Gas chemistry of the Ahuachapán and Berlin geothermal fields, El Salvador. Report 12 in: *Geothermal training in Iceland 2003*. UNU-GTP, Iceland, 275-304.

Karabelas, A.J., Andritsos, N., Mouza, A., Mitrakas, M., Vrouzi, F., and Christianis, K., 1989: Characteristics of scales from the Milos geothermal plant. *Geothermics, 18*, 169-174.

Kharaka, Y.K., Gunter, W.D., Aggarwal, P.K., Perkins, E.H., and Debraal, J.D., 1988: *SOLMINEQ.88: A computer program for geochemical modelling of water-rock interactions*. US Geological Survey books and open-file reports, 1988. 420 pp.

LaGeo, 2008: *Result on analysis. Main maintained Unit I. Ahuachapán geothermal field*. LaGeo S.A de C.V, internal report (in Spanish), 17 pp.

LaGeo, 2015: *Result on analysis. Main maintained Unit II. Ahuachapán geothermal field.* LaGeo S.A de C.V, internal report (in Spanish), 37 pp.

LaGeo, 2017a: *Central Ahuachapán geothermal field. Daily monitoring report*. LaGeo S.A de C.V, internal report (in Spanish), 6 pp.

LaGeo, 2017b: *Geothermal energy in El Salvador* (in Spanish). LaGeo, website: *www.lageo.com.sv*

Laky, C., Lippmann, M.J., Bödvarsson, G.S., Retana, M., and Cuellar, G., 1989: Hydrogeologic model of the Ahuachapán geothermal field, El Salvador. *Proceedings of the 14th Workshop on Geothermal Reservoir Engineering, Stanford University, California,* 265-272.

Montalvo L., F.E., 1994: Geochemical evolution of the Ahuachapán geothermal field, El Salvador C.A. Report 9 in: *Geothermal training in Iceland 1994,* UNU-GTP, Iceland, 211-236.

Montalvo, F.E., 2010: *Geothermal fields under exploitation in El Salvador. Actual status and development of geothermal resources in Central America* (in Spanish). DGCD/MAE, Pisa, Italy, 5079.

Padilla R., E.K., 2011: *Transport and precipitation of carbon and sulphur in the Reykjanes geothermal system, Iceland*. University of Iceland, MSc thesis, UNU-GTP, report 3, 48 pp.

Quijano C., J.E., 1994: A revised conceptual model and analysis of production data for the Ahuachapán-Chipilapa geothermal field in El Salvador. Report 10 in: *Geothermal training in Iceland 1994*, UNU-GTP, Iceland, 237-266.

Reed, M.H., and Palandri, J.L., 2006: Sulfide mineral precipitation from hydrothermal fluids. *Review in Mineralogy & Geochemistry, 61*, 609-631.

Simmons, S.F., and Brown, K.L.: The flux of gold and related metals through a volcanic arc, Taupo Volcanic Zone. Geology, 35: pp. 1099 – 1102. (2007)

Verma, M.P., 2012. Estimate of reservoir fluid characteristics as first step in geochemical modelling of geothermal systems. *Computers and Geosciences, 49,* 29-37.